IEEE Access
Multidisciplinary | Rapid Review | Open Access Journal

IEEE ON IEEE POWER & ENERGY SOCIETY SECTION

Received May 25, 2020, accepted June 24, 2020, date of publication June 30, 2020, date of current version July 20, 2020.

Digital Object Identifier 10.1109/ACCESS.2020.3006093

Charging Load Prediction and Distribution Network Reliability Evaluation Considering Electric Vehicles' Spatial-Temporal Transfer Randomness

SHAN CHENG[1,2], (Member, IEEE), ZHAOBIN WEI[1,2], DONGDONG SHANG[1,2], ZIKAI ZHAO[1,2], AND HUIMING CHEN[3]

[1]Hubei Provincial Collaborative Innovation Center for New Energy Microgrid, China Three Gorges University, Yichang 443002, China
[2]College of Electrical Engineering and New Energy, China Three Gorges University, Yichang 443002, China
[3]Department of Electrical and Electronic Engineering, The University of Hong Kong, Hong Kong

Corresponding author: Shan Cheng (hpucquyzu@ctgu.edu.cn)

This work was supported in part by the National Natural Science Foundation of China under Grant 51607105, and in part by the Research Fund for Excellent Dissertation of China Three Gorges University under Grant 2020SSPY059.

ABSTRACT Integration of large-scale cluster electric vehicles (EVs) and their spatial-temporal transfer randomness are likely to affect the safety and economic operation of the distribution network. This paper investigates the spatial-temporal distribution prediction of EVs' charging load and then evaluates the reliability of the distribution network penetrated with large-scale cluster EVs. To effectively predict the charging load, trip chain technology, Monte Carlo method and Markov decision process (MDP) theory are employed. Moreover, a spatial-temporal transfer model of EVs is established, and based on which, an EV energy consumption model and a charging load prediction model are constructed with consideration of temperature, traffic condition and EV owner's subjective willingness in different scenarios. With the application of sequential Monte Carlo method, the paper further evaluates distribution network reliability in various charging scenarios. In the evaluation, indices including per unit value (PUV), fast voltage stability index (FVSI), loss of load probability (LOLP), system average interruption frequency index (SAIFI), system average interruption duration index (SAIDI), and expected energy not supplied (EENS) are incorporated. To validate the proposed prediction model and evaluation method, a series of numerical simulations are conducted on the basis of taking the traffic-distribution system of a typical city as an example. The result demonstrates that the proposed spatial-temporal transfer model is more practical in charging load prediction than the popularly used Dijkstra's shortest path algorithm. Moreover, high temperature, congestion and the increment of EV penetration rate will further weaken distribution network reliability.

INDEX TERMS Electric vehicle, reliability evaluation, trip chain technology, Markov decision process, sequential Monte Carlo method, spatial-temporal transfer randomness.

NOMENCLATURE

ABBREVIATIONS

EV	Electric vehicle
MDP	Markov decision process
SOC	State of charge
TNN	Traffic network node
DNN	Distribution network node
DCP	Dispersion of charging power

PARAMETERS

μ	Mean of the beginning time of each trip
σ	Variance of the beginning time of each trip
$v_{\max}^{i,j}$	Maximum speed allowed at the road (i, j)
x	EV's position in the travel path
D^x	Distance between the origin of the trip and x
C_{EV}	Capacity of EV battery
$U_{sat}^{\min}$	Minimum value of U_{sat}
$U_{sat}^{\max}$	Maximum value of U_{sat}
p_{slow}	Rated power of slow charging

The associate editor coordinating the review of this manuscript and approving it for publication was Pierluigi Siano.

p_{fast}	Rated power of fast charging
soc^{i}_{init}	SOC of EV when arrived at the i_{th} charging station in a trip
soc_{exp}	Expected SOC of EV
soc_{thr}	Preset threshold of EV's SOC
T^{i}_{park}	Parking time of EV at the i_{th} charging station in a trip
D_{thr}	Distance that soc_{thr} can meet
$\|\|$	Or operation
N_{EV}	Total number of EVs connected to power grid
$p^{n}_{w}(t)$	Charging power for the n_{th} EV at DNN w
$P_{DN}(\text{t})$	Total charging power of EVs in distribution network
$\boldsymbol{W}$	Matrix composed of N_w rows and 96 columns
$P_{TG}(\text{t})$	Active power provided by the superior power supply to distribution network at time t
$P_{AL}(\text{t})$	Total power load of distribution network at time t

I. INTRODUCTION

With a new round of scientific and technological revolution and industrial transformation, the EV industry is entering a new stage of accelerated development. Especially in China, staying committed to sustainable development, the government has been making great efforts to speed up innovations of EV technologies and popularize the EVs [1]. However, the broadscale running of EVs is likely to result in significant impacts on both traffic network and distribution network [2], [3]. One key fundamental to ensure the positive effects of popularizing EVs is to effectively forecast the spatial-temporal distribution of EVs' charging load, while the other is to further evaluate the reliability of distribution network penetrated with large-scale cluster EVs.

Based on the National Household Travel Survey data released by the U.S. Department of Transportation, the fitting curves of departure time, connection time and daily mileage have been gained and then the EV charging load has been computed by Monte Carlo method in [4] and [5]. In [6] and [7], considering the stochastic nature of EVs moving, the spatial-temporal distribution characteristics of charging load of various types of EVs in different regions and periods have been studied. Further, Ul-Haq *et al.* [8] have explored the influence of drive intention of EV owners and electricity price on the spatial-temporal distribution of charging demand. These studies have established EV charging load model and analyzed its spatial-temporal distribution characteristics, but the EV locations and EV charging periods are fixed, which have failed to reflect the specific EV travel process and ignored the mobility of EVs.

Taking into account the fact that EVs are coupled with traffic network and distribution network simultaneously, Luo *et al.* [9] and Shao *et al.* [10] have constructed a fusion system integrated with "vehicle-traffic-distribution" and solved the spatial-temporal distribution of EV charging load by origin-destination matrix. In [11], a dynamic evolution model with EV spatial-temporal distribution has been proposed on the basis of cell agent theory and Dijkstra method. It aimed to plan EV trip path and predict EV charging load. Furthermore, considering traffic energy consumption and charging price, Chen *et al.* [12] have proposed a strategy to optimize EV trip path, which is on the basis of origin-destination matrix. Moreover, it acquires the charging load by mixed integer programming. The works above have built various spatial-temporal transfer models of EVs, which were based on the shortest path algorithm or aimed to optimize the EV path without taking into account traffic conditions [13].

Hence, to remedy the problem, trip chain theory has been employed to simulate EVs' dynamic driving process. To be specific, based on random trip chain and MDP theory, an EV spatial-temporal transfer model has been proposed in [14] and [15]. With the incorporation of stochastic trip chain, Tao *et al.* [16] have computed the spatial-temporal distributions of charging demands of EVs with the considerations of different dates and regions. Besides, Markov chain Monte Carlo method has been used to simulate EV travel and charging behavior in [17]. Despite the effectiveness and advantages of the EV travel models presented in [14]–[17], various environmental factors, including temperature, traffic congestion and subjective charging willingness, have not been considered in the prediction of EVs' charging load. It should be noted that on high temperature day, EV users probably turn on air conditioning, causing at least 20% increment in electricity consumption [18]. Furthermore, traffic congestion can affect charging behaviors and lead to the variance of connection periods [19]. In addition, the subjective charging willingness of EV users can give birth to extra charging demand [20]. Hence, these factors are of great significance for the prediction accuracy of charging load and shall be carefully studied.

Besides, it has been shown that the uncertain characteristics of EVs charging would be adverse to power system reliability [21]. Thus, it is necessary to evaluate distribution network reliability with the integration of EVs. Specifically, Kamruzzaman and Benidris [22] have calculated the load loss of distribution network with the maximum permissible penetration level of EVs. In [14] and [23], different EV penetration rates have been employed to compute corresponding charging demand. Further, Wang and Infield [17] have discussed the impact of various EV penetration levels on the thermal performance of substation feeders. To reduce the cost of EV aggregators and improve operators' technical problems, Clairand *et al.* [24] have proposed a smart charging method with the deployment of different EV penetration levels. It should be noted that the main ingredient among [14], [17] and [22]–[24] is that they all have investigated the impact of EV penetration level on power system. However, all of the above works lack the systematic evaluation in the influence of the variance of EV penetration rates on distribution network reliability, which may create a barrier for the safe operation of distribution system.

Apart from this, Liu *et al.* [25] have carried out generation adequacy analysis in light of the connection of EVs.

In [26] and [27], analytical methods have been proposed, and the main ingredient is to assess the impact on grid reliability caused by large-scale EVs integration. With the application of quasi-dynamic simulation method, Zhang *et al.* [28] have studied the influence of EVs penetration and their battery capacities on the reliability of distribution network. However, these works have failed to quantitively analyze the impact of EVs charging load on the distribution network reliability resulting from high temperature and congestion.

Subsequently, to address the aforementioned problems with the above considerations, a novel method of EVs charging load prediction has been proposed. Specifically, the proposed method has taken into account the spatial-temporal transfer randomness in vehicle-road-grid mode. Moreover, the reliability of distribution network penetrated with large-scale EVs has been further evaluated. The main contributions of the paper can be summarized as follows:

1) A novel spatial-temporal transfer model: a novel spatial-temporal transfer model for urban EVs has been proposed. To be technically precise, the methods of trip chain, Monte Carlo and MDP for the novel model have been incorporated. Compared with the popularly used Dijkstra's shortest path algorithm, the proposed model has fully reflected the randomness of EV's movement, which shall make it substantially more accurate in real applications.

2) A novel method for charging load prediction: Taking into account temperature, traffic condition and EV owner's subjective willingness, a novel method of charging load prediction has been proposed. Particularly, the method can be employed in different scenarios, including weekday, weekend, high temperature day and congestion day.

3) The comprehensive study on the effect of different scenarios of reliability evaluation: to be specific, the impact of charging load caused by various EV penetration rates, high temperature and congestion on distribution network reliability has been extensively studied. In particular, except for the reliability indices including PUV, LOLP, SAIFI, SAIDI and EENS, FVSI has been further proposed to reflect the voltage stability of distribution network.

The rest of the paper is organized as follows: Section II describes the EV spatial-temporal transfer model and energy consumption computation process in detail, so as to calculate charging load. In Section III, the reliability evaluation of distribution network in different charging scenarios of EVs has been fully investigated. Furthermore, the comparison and analysis of numerical simulation have been conducted in section IV. Finally, conclusion is drawn in section V.

II. SPATIAL-TEMPORAL TRANSFER MODEL AND CHARGING LOAD CALCULATION

In this section, the spatial-temporal transfer model is introduced. In traditional transfer models, the shortest path planning algorithm such as Dijkstra is often applied to simulate EVs' driving path. However, due to the reason that EV users may be affected by multiple environmental factors when making path decisions, this kind of algorithm may fail to reflect the randomness of EVs mobility. Therefore, a novel spatial-temporal transfer model to address the problem has been proposed. The main ingredient is that the proposed model has incorporated trip chain, MDP and Monte Carlo method. On the basis of the proposed model, the EV charging load prediction is further conducted.

A. EV TRAVEL MODEL

In general, EV travel destinations can be divided into five categories, home (H), working unit (W), shopping and eating places (SE), social and entertainment places (SR) and others (O). It should be emphasized that these locations are also provided with EV charging services. As shown in Figure 1, the trip chain mainly consists of three types, including H-W, H-SR/SE/O and H-W-SR/SE/O. In addition, the composition and proportion of the trip chains are different on weekdays and weekends, which are listed in Table 1 as follows [28]:

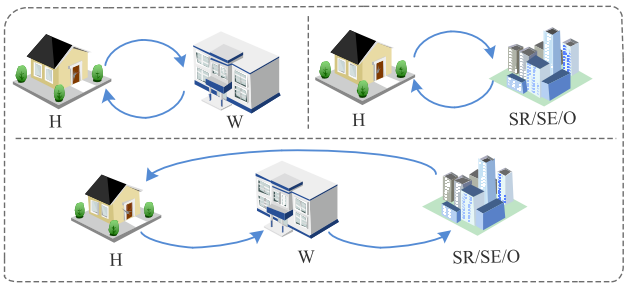

FIGURE 1. Trip chain structure.

TABLE 1. Trip chain composition and proportion on weekdays and weekends.

Scenario day	Trip chain	Chain number	Ratio/%
Weekdays	H-W	1	52.8
	H-W-SR/SE/O	2	24.1
	H-SR/SE/O	3	23.1
Weekends	H-SR/SE/O	4	35
	H-SR/SE/O	5	35
	No trip	6	30

Specifically, the beginning time t_s of each trip follows the normal distribution, with probability density function $f(t_s)$ given as follows [29]:

$$f(t_s) = \frac{1}{\sqrt{2\pi}\sigma} \exp(-\frac{(t_s - \mu)^2}{2\sigma^2}). \quad (1)$$

The value of μ and σ varies with trip chains, and different scenarios and choices can be obtained in Table 2.

B. SIMULATION OF EV RANDOM PATH BASED ON MDP

The EV travel model has been discussed in the last subsection, next the EV path simulation based on MDP is to be explained. Specifically, since the travel path of EVs can directly affect the spatial-temporal distribution of charging load, MDP is employed to simulate the travel path of EVs. Subsequently, standard MDP model can be described by a

TABLE 2. The probability distribution of different trip chains.

Scenario day	Chain number	A.M.	P.M.
Weekdays	1	N(6.92,1.24)	N(17.47,1.80)
	2	N(6.92,1.24)	N(17.47,1.80)
	3	N(8.98,3.24)	-
	4	N(8.98,3.24)	-
Weekends	5	-	N(16.47,3.41)
	6	-	-

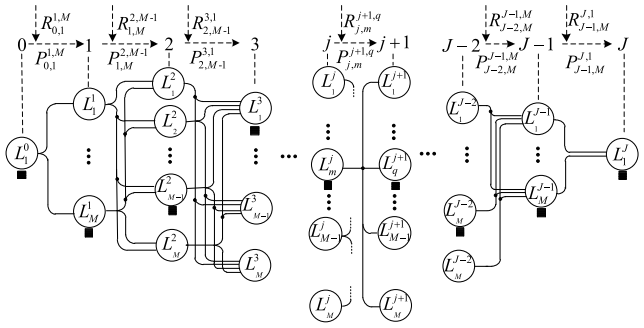

FIGURE 2. Schematic diagram of the transportation network.

five-element group {**T**, **S**, **A**, **P**, **R**} [30]. The application is illustrated in Figure 2.

Here, the parameters are illustrated as follows:

a) **T** represents the decision time set in a trip chain. In a trip with J locations, $t_j \in \mathbf{T}$ is the moment when an EV has passed j locations or started with the $j+1$ location, $j \in \{0, 1, 2, \ldots, J-1\}$.

b) **S** denotes the state space set in a trip chain. For a transportation network with L locations, $s_j \in \mathbf{S}$ indicates the EV's location at t_j.

c) **A** prescribes the action sets in a trip chain, indicating the possible optional actions made at each decision-making time. In addition, a policy π means a set of ordered decisions from t_0 to t_{J-1}, which can be expressed by $\pi = \{\pi(s_j), j = 0, 1, 2, \ldots, J-1, s_j \in \mathbf{S}\}$. In other words, a policy π can directly represent the specific path in a trip chain. In Figure 2, the black blocks show where an EV travels, i.e., the policy π or the EV's path can be listed as $\{L_1^0, L_M^1, L_{M-1}^2, L_1^3, \ldots, L_m^j, L_q^{j+1}, \ldots, L_{M-1}^{J-2}, L_M^{J-1}, L_1^J\}$, M is the total number of locations that can be selected when the EV is at the j_{th} location.

d) It should be noted that a transition probability is needed to embody the possibility of an EV moving from one TNN to another one. To be specific, let **P** denote the set of state transition probability. When an EV makes a path selection action at time t_j, it will move from current state s_j to another state s_{j+1}. Subsequently, the transition probability between the two states can be expressed as:

$$p^a_{j,j+1} = P(S = s_{j+1} | S = s_j \cap \pi(s_j) = a). \tag{2}$$

In the simulation of EVs random path, if $s_j = L_m^j$, the state transition probability can be derived. To be precise, let $G_{j,m}^{j+1,q}$ and $V_{j,m}^{j+1,q}$ denote the distance and speed between location L_m^j and L_q^{j+1}, respectively, with m and $q \in \{1, 2, \ldots, M\}$. If the EV can reach the next location L_{st}^{j+1} with the shortest time, the transition probability is set to be $P_{j,m}^{j+1,st}$, which is bigger than the other transition probabilities in the same state, here $st \in \{1, 2, \ldots, M\}$. Then the selection probability $P_{j,m}^{j+1,q}$ is determined according to EV's driving time between L_m^j and L_q^{j+1}. The principle is that longer the driving time leads to the smaller the transition probability, thus the probability can be expressed as:

$$\begin{cases} P\_t_{j,m}^{j+1,q} = 1 & M = 1 \\ P\_t_{j,m}^{j+1,q} = \dfrac{\sum_{k=1}^{M} \dfrac{G_{j,m}^{j+1,k}}{V_{j,m}^{j+1,k}} - \dfrac{G_{j,m}^{j+1,q}}{V_{j,m}^{j+1,q}}}{(M-1)\sum_{k=1}^{M} \dfrac{G_{j,m}^{j+1,k}}{V_{j,m}^{j+1,k}}} & M \geq 2 \\ P\_t_{\max} = \max(P\_t_{j,m}^{j+1,k}), \end{cases} \tag{3}$$

$$\begin{cases} P_{j,m}^{j+1,q} = 1 & M = 1 \\ P_{j,m}^{j+1,q} = \dfrac{(1 - P_{j,m}^{j+1,st}) G_{j,m}^{j+1,q}}{(1 - P\_t_{\max}) V_{j,m}^{j+1,q}} & M \geq 2, q \neq st. \end{cases} \tag{4}$$

e) Next, let R denote the reward set in a trip chain, which is used to evaluate the advantage or disadvantage of EV actions (i.e. path selection). In this paper, R refers to the driving time of EVs. For instance, if an EV transfers from L_m^j to L_q^{j+1} with transition probability $P_{j,m}^{j+1,q}$, the action will be evaluated as reward $R_{j,m}^{j+1,q}$, as demonstrated in Figure 2. Note that the greater the reward is, the shorter the driving time will be.

It is noteworthy that both **P** and **R** have a correlation with driving time. The internal link between **P** and **R** is a causal relationship. To acquire the maximum possible reward, the transition probability of the path with the shortest driving time is set bigger than that of others. In this way, both transition randomness and optimal path (i.e. the least time consuming path) have been taken into consideration in path simulation, which is more realistic.

C. COMPUTATION MODEL OF ELECTRICITY CONSUMPTION PER KILOMETER

In the urban traffic system, EVs' speed is mainly affected by road capacity and vehicle flow. To simulate the actual EV speed within a day, a speed-flow model is introduced [31]. Specifically, let $v_t^{i,j}(x)$ denote the EV speed at x on a directly connected road, where i and j are the two ends of the road, respectively. Here, $v_t^{i,j}(x)$ can be computed via (5):

$$\begin{cases} v_t^{i,j}(x) = \dfrac{v_{\max}^{i,j}}{1 + \chi_t^{\beta}} \\ \beta = \alpha_1 + \alpha_2 \cdot \chi_t^{\alpha_3} \\ \chi_t = \dfrac{d_t^{i,j}(x)}{Tr^{i,j}}, \end{cases} \tag{5}$$

where: α_1, α_2 and α_3 are adaptive coefficients; $d_t^{i,j}(x)$ is the traffic flow at x of the road (i, j), and $Tr^{i,j}$ represents the traffic

capacity of the road; χ_t denotes the saturation degree of a road at time t, which is the result of $d_t^{i,j}(x)$ divided by $Tr^{i,j}$. It should be noted that χ_t is directly given out in Table 4 to simplify the calculation [32].

Traditionally, EV electricity consumption per kilometer at x, i.e., $E_t^{i,j}(x)$, can be obtained via (6) [33].

$$E_t^{i,j}(x) = -0.179 + 0.004v_t^{i,j}(x) + \frac{5.492}{v_t^{i,j}(x)}. \tag{6}$$

Additionally, the electricity consumption increases with working air-conditioning because of high and low temperatures. Therefore, incorporate another two parameters, namely the probability of air-conditioning turning on K_{pect} and energy proportion coefficient K_{temp} to compute the energy consumption with different temperatures:

$$\begin{cases} K_{pect} = k_1U^3 + k_2U^2 + k_3U + c_1 \\ K_{temp} = k_4(U + c_2)^2 + c_3, \end{cases} \tag{7}$$

where: $k_1 \sim k_4$ and $c_1 \sim c_3$ are constant values; U denotes temperature. In particular, K_{pect} under different temperatures is depicted in Figure 3. Moreover, the on-off decision for air-conditioning is necessary to be discussed. Generate a random number r submitted to uniform distribution for a certain temperature. If $r < K_{pect}$ is satisfied, turn on air-conditioning. Otherwise, air-conditioning remains off.

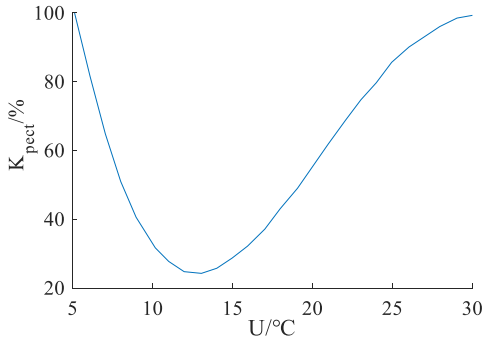

FIGURE 3. K_{pect} under different temperatures.

Consequently, the electricity consumption per kilometer at x considering the impact of air-conditioning, i.e. $E_t(x)$, can be derived more accurately via (8):

$$E_t(x) = \begin{cases} K_t^{temp}E_t^{i,j}(x) & r \le K_{pect} \\ E_t^{i,j}(x) & r > K_{pect}. \end{cases} \tag{8}$$

Subsequently, the actual SOC of EVs at location x can be further acquired as follows:

$$soc_x = (soc_{init} - \frac{\int_0^{D^x} E_t(x)d_x}{C_{EV}}) \times 100\%, \tag{9}$$

where d_x represents an infinitesimal distance.

It should be noted in (9) that the SOC in the form cannot be directly applied. Hence, in this paper, it is discretized for the fact that the accuracy of x is 1 km. Subsequently, the equation in (9) is approximated as follows:

$$soc_x = (soc_{init} - \frac{\sum_0^{D^x} E_t(x)}{C_{EV}}) \times 100\%. \tag{10}$$

D. CHARGING DEMAND CONSIDERING EV OWNER'S SUBJECTIVE WILLINGNESS

Now turn the attention to the charging demand. To start with, the EV charging behavior is divided into two categories:

1) The SOC of an EV cannot guarantee the remaining distance, and the EV owner chooses to charge at the current charging station.

2) The remaining electricity is enough but the EV gets charged at the end of the trip due to the owner's anxiety about the next trip. If the anxiety turns up, the owner will choose to charge the EV out of subjective willingness. Moreover, there is a negative correlation between the subjective willingness of EV owner and EV's SOC at the end of the finished trip, i.e., the decrement of the latter will lead to the increment of the former.

Additionally, the fuzzy theory is adopted and the index "electricity satisfaction degree U_{sat}" is employed to describe the subjective willingness of EV owner to charge as follows:

$$U_{sat} = \frac{soc_x C_{EV}}{\sum_0^{D_{next}} E_t(x)}, \tag{11}$$

where: D_{next} denotes the distance of EV's next trip.

Let F_{fuz} denote the fuzzy set of charging demand, then its membership function $F_{fuz}(U_{sat})$ can be expressed as follows [20]:

$$F_{fuz}(U_{sat}) = \begin{cases} 1 & U_{sat} < U_{sat}^{\min} \\ \tau & U_{sat}^{\min} \le U_{sat} < U_{sat}^{\max} \\ 0 & U_f \ge U_{sat}^{\max}, \end{cases} \tag{12}$$

$$\tau = \sin[\frac{\pi}{4}(1 + \frac{U_{sat}^{\min}}{2}(\frac{U_{sat}^{\max} - 2U_{sat} + U_{sat}^{\min}}{U_{sat}^{\max} - U_{sat}^{\min}}))]. \tag{13}$$

In (12), $F_{fuz}(U_{sat})$ indicates the charging probability of EV owner, which can explicitly quantify the referred anxiety about the next trip. To be precise, if $U_{sat} < U_{sat}^{min}$, there must be charging demand for the reason that EV's remaining electricity cannot meet the following trip. Conversely, if $U_{sat} \ge U_{sat}^{max}$, the charging probability decreases to 0 because the EV has enough power to complete the next trip. Further, if U_{sat} stays between $U_{sat}^{\min}$ and $U_{sat}^{\max}$, the charging probability τ is determined via (13).

Once charging demand is confirmed, the EV owner needs to choose charging mode which is mainly divided into slow charging and fast charging [34]. Considering the charging cost and battery loss, slow charging is the default option. However, if the EV's SOC cannot reach the preset expectation within the parking time, which is described in (14), fast

charging will be chosen:

$$\frac{P_{slow}T_p^i}{C_{EV}} + soc_{init}^i < soc_{\exp}. \tag{14}$$

Furthermore, when the EV SOC on passage is lower than soc_{thr}, the EV will choose to charge at a certain charging station L_{par}^{mid}, and the charging time T_{char} is further determined. Specifically, L_{par}^{mid} and T_{char} are given as follows:

$$\begin{cases} \sum_{0}^{D_{thr}} E_t(x) = C_{EV}(soc_{init} - soc_{thr}) \\ \sum_{r=1}^{r_c} D_r < D_{thr}, \quad r_c \in \{1, 2, \ldots, J\} \\ L_{par}^{mid} = f(r_c), \end{cases} \tag{15}$$

$$\begin{cases} D_{mid} = \sum_{r=1}^{r_c} D_r \\ T_{Char} = \dfrac{\sum_{0}^{D_{mid}} E_t(x) - soc_{init} C_{EV}}{(p_{fast}||p_{slow})}, \end{cases} \tag{16}$$

where: D_{thr} means the distance that the EV drives from soc_{ini} to soc_{thr}; $\sum D_r$ is the distance between the origin of the trip and the r_{th} charging station that the EV has passed by; r_c is the number of charging stations that the EV has passed by when the SOC of EV decreases to soc_{thr}; $f(r_c)$ means the TNN corresponding to r_c.

E. IMPACT OF $P_{j,m}^{j+1,st}$ ON THE SPATIAL-TEMPORAL DISTRIBUTION OF CHARGING LOAD

In this subsection, the impact of probability $P_{j,m}^{j+1,st}$ on the spatial-temporal distribution of charging load will be fully investigated for the reason that $P_{j,m}^{j+1,st}$ can change the driving path results. To embody the dispersion characteristic of charging load in a whole area l (i.e. residential area (RA), commercial area (CA) or working area (WA)), index I_{DCP}^l is proposed and can be identified via (17) and (18) as follows:

$$I_{DCP}^l = \frac{\sum_{t=1}^{T} \sum_{w^l}^{N_w^l} (P_w^l(t) - P_w^{avr})^2}{\sum_{t=1}^{T} \sum_{w^l}^{N_w^{all}} P_w^l(t)}, \tag{17}$$

$$P_w^{avr} = \frac{\sum_{t=1}^{T} \sum_{w^l}^{N_w^{all}} (P_w^l(t))}{N_w^{all} T}. \tag{18}$$

where: N_w^l is the total number of TNN in area l; $P_w^l(t)$ denotes the charging load of TNN w^l; N_w^{all} means the total number of TNN in all the three areas; P_w^{avr} is the average charging load in all the three areas. In general, the essence that I_{DCP}^l can reflect the dispersion characteristecs of charging load is because I_{DCP}^l is determined by the sum of the differences between $P_w^l(t)$ and P_w^{avr}.

F. CHARGING LOAD CALCULATION OF DISTRIBUTION NETWORK

It is needed to gather the charging load information of the whole system. Firstly, compile statistics of the spatial-temporal information of each DNN according to the coupling relationship between TNN and DNN. Subsequently, the charging load of DNN w can be expressed as:

$$P_w(t) = \sum_{n=1}^{N_{EV}} P_w^n(t). \tag{19}$$

Furthermore, the total charging load of distribution network $P_{DN}(t)$ can be gained via (20):

$$P_{DN}(t) = \sum_{w=1}^{N_w} p_w(t). \tag{20}$$

For the stopping criterion, let $P_{DN}(t)$ store in $\boldsymbol{W}$. Then, when the number of simulations y_1 reaches the maximum value Z_1 or meets the convergence criterion (21) [35], the simulation is terminated. Otherwise, repeat charging load prediction.

$$\max\{|A_n^{W_b} - A_{n-1}^{W_b}|\} \le \zeta_1. \tag{21}$$

where: $\boldsymbol{W_b}$ is the b_{th} column vector in matrix $\boldsymbol{W}$; A_n^{Wb} denotes the mean value of $\boldsymbol{W_b}$ in the n_{th} simulation; ζ_1 is the convergence accuracy in the simulation. Figure 4 displays the charging load calculation in detail.

III. RELIABILITY EVALUATION OF DISTRIBUTION NETWORK

The charging load prediction has been studied in the previous section. In summary, the charging load prediction enjoys high prediction accuracy with consideration of multiple realistic environmental factors. In this section, the impact of predicted charging load on distribution network reliability will be mainly analyzed. Specifically, factors including EV penetration rate, temperature and traffic congestion will be comprehensively taken into account.

A. RELIABILITY EVALUATION INDICES OF DISTRIBUTION NETWORK

Firstly, a series of indices are adopted to evaluate the distribution network reliability which is demonstrated as follows [36], [37]:

1) Per unit value (PUV) is given as follows:

$$I_{PUV} = \frac{V_i - V_i^{ra}}{V_i^{ra}} \times 100\%, \tag{22}$$

where: V_i is the real-time voltage at the i_{th} node; V_i^{ra} denotes the rated voltage at the i_{th} node.

2) Fast voltage stability Index (FVSI) is yielded:

$$I_{FVSI} = \frac{4(Z_{ij})^2 Q_j}{(V_i)^2 X_{ij}}, \tag{23}$$

where: Z_{ij} and X_{ij} denote the transmission line impedance and reactance, respectively; Q_j means reactive power at the receiving end.

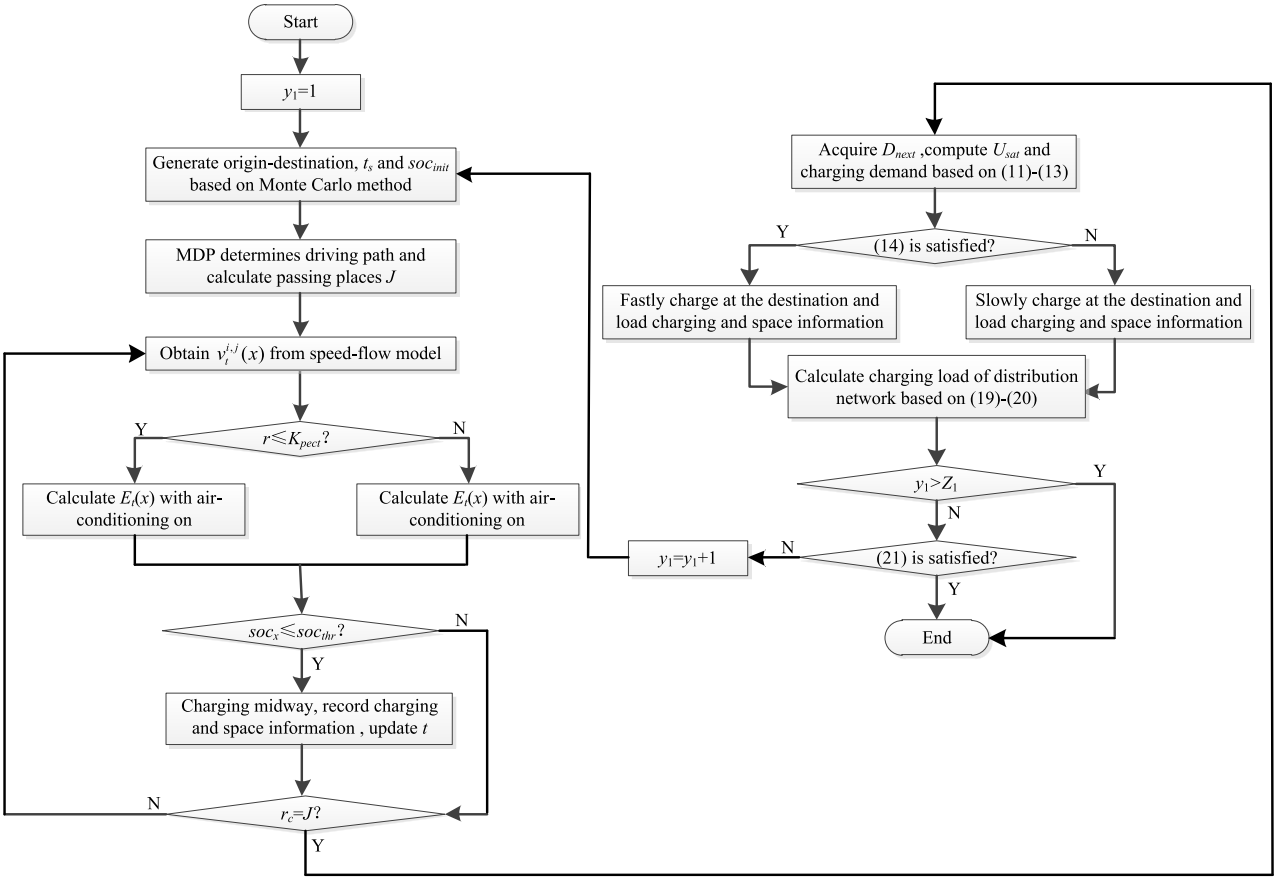

FIGURE 4. Charging load calculation flowchart.

3) Loss of load probability (LOLP) can be obtained as follows:

$$I_{LOLP} = \frac{1}{T_{total}} \sum_{n_b=1}^{N_b} T_{bre}^{n_b}, \tag{24}$$

$$T_{total} = \sum_{n_b=1}^{N_b} (T_{norm}^{n_b} + T_{bre}^{n_b}), \tag{25}$$

where: N_b is the total simulation times; T_{norm}^{nb} and T_{bre}^{nb} denote the fault period and normal period, respectively; T_{total} is the total period of N_b simulations.

4) System average interruption frequency index (SAIFI) is presented as follows:

$$I_{SAIFI} = \frac{\sum_{n_b=1}^{N_b} \sum_{w}^{N_w} F_{n_b}^{w}}{N_R N_w}, \tag{26}$$

where: N_R represents the total years applied for reliability evaluation; F_{nb}^{w} denotes the interruption time at DNN w.

5) System average interruption duration index (SAIDI) is provided:

$$I_{SAIDI} = \frac{\sum_{n_b=1}^{N_b} \sum_{w}^{N_w} T_{bre}^{n_b,w}}{N_R N_w}. \tag{27}$$

6) Expected energy not supplied (EENS) is derived:

$$I_{EENS} = \frac{1}{N_R} \sum_{n_b=1}^{N_b} \sum_{w=1}^{N_w} E_{n_b}^{w}, \tag{28}$$

where: E_{nb}^{w} is the load loss at DNN w in the n_{b_th} simulation.

B. RELIABILITY EVALUATION PROCESS BASED ON SEQUENTIAL MONTE CARLO

Next, continue to study the specific process of reliability evaluation. In the distribution network, each component has a failure rate λ and repair rate ρ. On the basis of this, employ sequential Monte Carlo method to sample the component sequence in the process of ''Normal-Fault-Normal''. Assume that the duration of every component in each state follows the exponential distribution [38]:

$$\begin{cases} H(\lambda) = \lambda e^{-\lambda \upsilon_1} \\ \upsilon_1 = \dfrac{1}{\lambda} \ln \varphi_1 \\ H(\rho) = \rho e^{-\rho \upsilon_2} \\ \upsilon_2 = \dfrac{1}{\rho} \ln \varphi_2, \end{cases} \tag{29}$$

where: φ_1 and φ_2 are both random numbers between 0 and 1.

Now it is in the position to discuss the calculation procedure. According to the component state sequence and state

duration, the operation state of the whole system can be obtained. After that, the reliability indices are calculated according to the equations (22)-(28). In general, it takes 5 years as the simulation period to evaluate the reliability of the system. For convenience, summarize the computation steps as follows:

1) Input the original data of the system, including the topological connection relationship of distribution network, basic load of each node and EVs charging load.

2) Sample the state sequence and state duration of components so as to obtain the operation state of the system.

3) Judge whether the system state is in fault or satisfies the condition listed in (30). If it is, calculate the system power flow and the optimal load reduction:

$$P_{TG}(t) < P_{AL}(t). \tag{30}$$

4) When the number of simulations y_2 reaches the maximum value Z_2 or the convergence condition equation (31) is satisfied, terminate the simulation [35]:

$$\eta = \frac{\sqrt{I(v_{Zi})}}{U[v_{Zi}]} \leq \zeta_2, \tag{31}$$

where: η is a variance coefficient; $I(\cdot)$ denotes variance function; $U[\cdot]$ prescribes the parameter expectation; v_{Zi} means the estimation of reliability indices after Zi simulations. And ζ_2 indicates the convergence accuracy in the simulation.

IV. CASE STUDIES AND ANALYSIS

The method of charging load prediction and reliability evaluation of distribution network have been elaborated. In this section, comprehensive experiments are conducted to verify the effectiveness of the proposed method. To be technically precise, take a typical urban traffic network as an example, the simulation of EV charging load in this area is conducted and then the corresponding results are discussed. The regions in the traffic network are mainly divided into RA (including TNN 1 to TNN 17), WA (including TNN 18 to TNN 22) and CA (including TNN 23 to TNN 30). The coupling between TNN and DNN is listed in Table 3. Road saturation in each period and the road length are displayed in Table 4 and Table 5, respectively. In addition, the transportation system consists of 30 TNNs and 52 roads, which all belong to urban trunk roads so as to simplify the calculation complexity and improve simulation efficiency. In regards to the structure of distribution network, IEEE 33-bus system is adopted, where 6 positions are equipped with sectionalized switches. The topology between traffic network and distribution network is illustrated in Figure 5. Each switch is with a failure rate of 0.0006 and an average repair time of 0.5h. For the feeders, the failure rate and average repair time are 0.002 and 2h, respectively.

In the simulation, the total number of EVs in the traffic network is 15000, and all EVs are under the same specification where C_{EV} is 32 kWh [39]. Additionally, p_{slow} and p_{fast}

TABLE 3. Coupling between TNN and DNN.

TNN	DNN	TNN	DNN	TNN	DNN
1	1	12	12	23	4
2	2	13	13	24	9
3	3	14	14	25	11
4	6	15	15	26	25
5	24	16	16	27	26
6	19	17	29	28	10
7	20	18	28	29	8
8	21	19	5	30	7
9	22	20	23	31	-
10	30	21	18	32	-
11	17	22	27	33	-

TABLE 4. Road saturation within a day.

Period	χ_t	Period	χ_t
00:00—07:00	0.2	14:00—17:00	0.3
07:00—09:00	0.5	17:00—19:00	0.5
09:00—12:00	0.3	19:00—23:00	0.3
12:00—14:00	0.4	23:00—24:00	0.2

TABLE 5. Road length.

Road	Length/ km	Road	Length/ km	Road	Length/ km
(1,2)	10.2	(9,11)	10.1	(18,27)	9.7
(1,4)	10.4	(10,11)	9.0	(19,20)	10.0
(2,3)	10.3	(10,21)	10.1	(19,24)	10.4
(2,5)	10.5	(11,22)	10.2	(19,28)	8.8
(2,6)	10.6	(12,13)	10.3	(20,21)	9.1
(3,4)	10.4	(12,16)	10.6	(20,25)	10.5
(3,7)	10.7	(12,17)	10.7	(20,29)	8.9
(4,8)	10.8	(13,14)	10.4	(21,22)	10.2
(4,9)	9.9	(13,15)	10.5	(21,25)	10.5
(5,6)	10.6	(14,15)	9.5	(22,30)	11.0
(5,23)	10.3	(14,28)	9.7	(23,24)	10.4
(6,7)	9.7	(15,16)	8.6	(24,25)	9.5
(6,24)	9.4	(15,28)	8.8	(25,26)	9.6
(7,8)	10.8	(16,17)	10.7	(27,28)	9.8
(7,25)	9.5	(16,29)	8.9	(28,29)	8.9
(8,10)	10.0	(17,30)	11.0	(29,30)	11.0
(8,26)	9.6	(18,19)	8.9	-	-
(9,10)	9.9	(18,23)	10.3	-	-

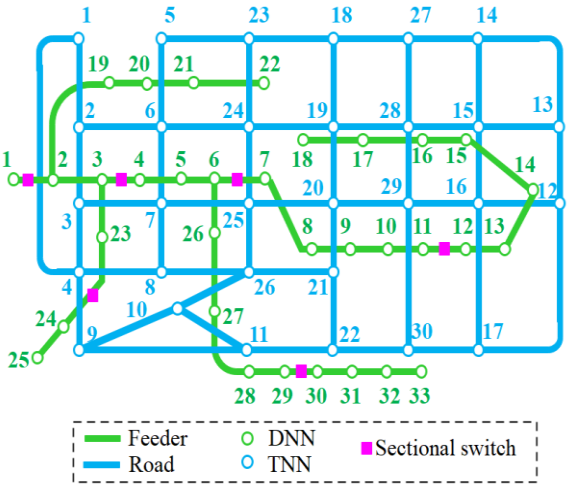

FIGURE 5. Topology between traffic network and IEEE 33-bus system.

are 7kW/h and 30kW/h, respectively. Furthermore, soc_{init} is randomly distributed between 0.85 and 1 and is generated by Monte Carlo method. And U_{sat}^{min} and U_{sat}^{max} are set to be 1.2 and 2, respectively.

A. SPATIAL-TEMPORAL DISTRIBUTION OF CHARGING LOAD IN WEEKDAY AND WEEKEND

The charging load on weekday and weekend is conducted numerically in the simulation, as illustrated in Figure 6. The results demonstrate that during the weekday, the peak period in WA mainly drops in 09:00 to 12:00, while that in RA and CA is from 18:00 to 22:00. In other time slots, the charging load of all the three areas keeps close to zero. Conversely, on weekend, charging power in WA stays almost zero and that of the other two areas performs more uniformly from 09:00 to 24:00. This temporal distribution is mainly determined by the structure and trip time of trip chains, as shown in Table 1 and Table 2. It can be concluded that the peak periods of the three areas on weekday and weekend are all 1 to 3 hours later than the beginning time of actual trips. Moreover, the time difference is mainly caused by transportation between different destinations. Additionally, the peak of charging load on weekday is almost 1.5 times bigger than that on weekend. This can be attributed to the fact that 30% of the total EVs on weekend are not used for transportation, which causes no charging demand for the system.

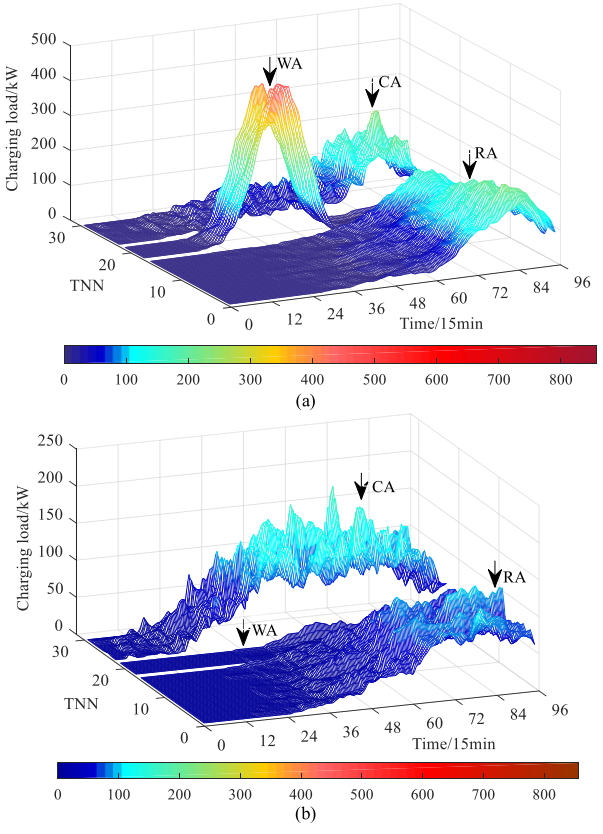

FIGURE 6. Charging load on weekday and weekend. (a) Weekday. (b) Weekend.

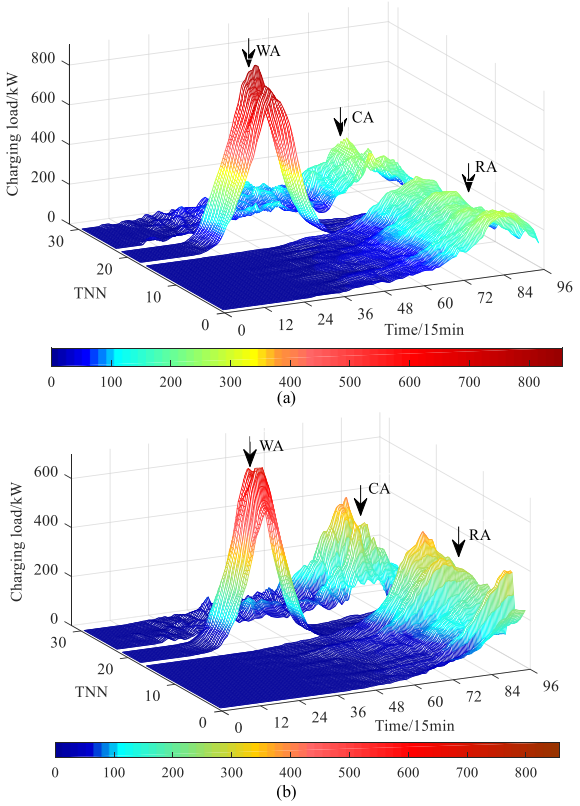

FIGURE 7. Charging load on high temperature day and congestion day. (a) High temperature day. (b) Congestion day.

B. SPATIAL-TEMPORAL DISTRIBUTION OF CHARGING LOAD ON HIGH TEMPERATURE DAY AND CONGESTION DAY

To investigate the impact of temperature and traffic condition on charging demand, the charging load on high temperature day and congestion day is performed and the results are depicted in Figure 7. It is worthwhile pointing out that the parameters used for high temperature day and congestion day are almost the same as those of weekday except temperature and EVs' driving speed. It can be seen that the spatial-temporal distribution of charging load on high temperature day is similar to that of weekday. However, the overall amplitude of the former increases dramatically, whose peak exceeds 80.59% of the peak of the latter. This is mainly due to the reason that the electricity is not only used for transportation, but also for air-conditioning working on high temperature day. Moreover, compared with the charging load on weekday, the peak of charging load on congestion day has increased by 52.32%, and time latency of charging load in RA and CA has happened. This is because congestion will result in cluster EVs' spending more time on transportation and charging.

C. CHARGING LOAD OF WEEKDAY BY THE SHORTEST PATH

Next, to clearly show the difference from the charging load by random path on weekday, the shortest path planning method

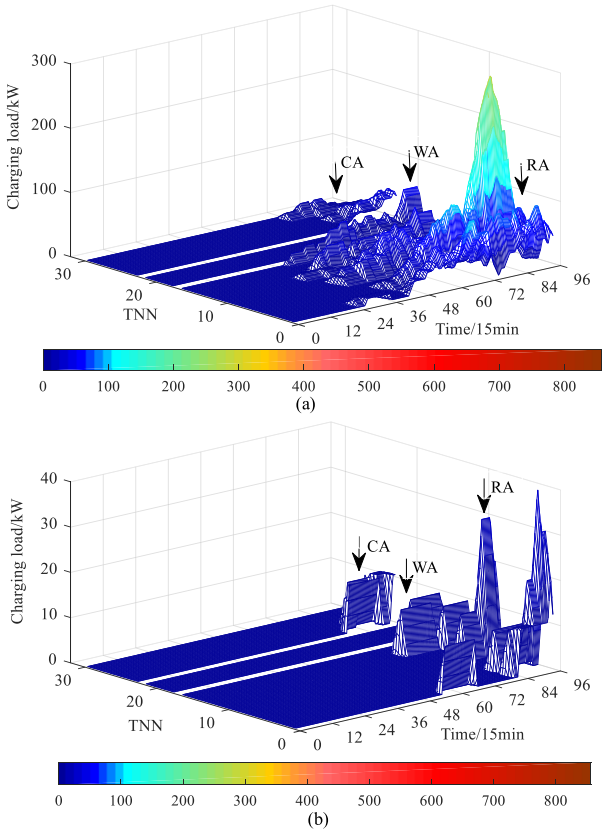

FIGURE 8. Charging load of weekday by the shortest path. (a) With subjective charging willingness. (b) Without subjective charging willingness.

(i.e. Dijkstra algorithm) is employed in the experiments and the results are illustrated in Figure 8(a). It can be obtained that the spatial-temporal distribution is completely different from that by MDP. The charging load in CA and WA remains lower than 100 kW, which is much fewer than that by MDP illustrated in Figure 6(a). Furthermore, the charging load mainly centers at RA after 20:00. The overall amplitude has decreased sharply and the peak of charging load by Dijkstra has decreased by 28.4% compared with that by MDP. The reason lies in the fact that EVs' electricity consumption caused by Dijkstra is fewer than that by MDP, which can be generally satisfied by soc_{init}. Consequently, the frequency of charging within a day will be cut down. Moreover, only a few EVs choose to charge in RA when getting back home after the day's trip. In addition, to demonstrate the necessity of subjective charging willingness, Figure 8(b) gives the case for the charging load without considering this factor. The spatial-temporal distribution is roughly the same as that considering subjective charging willingness, charging load in which also concentrates in RA during the period of 20:00-24:00. However, it can be seen that a significant drop occurs to the overall charging load of the former, and the peak load only accounts for 13.51% of that in the latter. This indicates the fact that subjective charging willingness plays an important role in guaranteeing the prediction accuracy of charging load.

D. FAST CHARGING TIMES OF CA IN DIFFERENT SCENARIOS

Generally, the probability of fast charging in CA is much bigger than that in RA and WA. This is because T_{char} in CA is too short to satisfy EVs' power expectation. Moreover, it is helpful for the operation of charging station to figure out the fast charging times of CA in different scenarios, as illustrated in Figure 9. On weekdays, the fast charging times are mainly from 18:00 to 21:00, due to the entertainment activities after work. On the contrary, on weekend, fast charging is more scattered in the period of 14:00 to 19:00. Moreover, the period distribution of fast charging on high temperature day and congestion day is similar to that on weekdays. However, the peak number of the two kinds of days increases dramatically because of increasing charging demand.

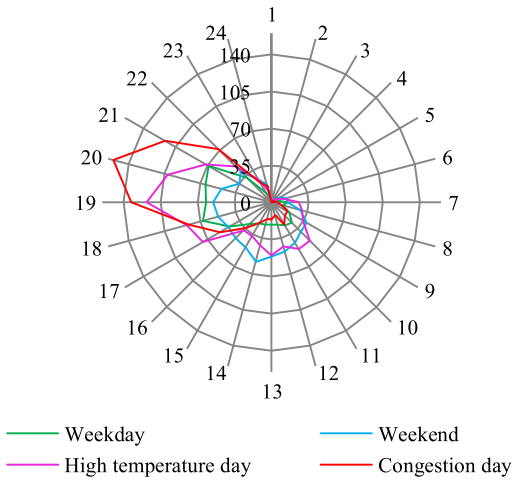

FIGURE 9. Fast charging times of CA in different scenarios.

E. STATISTICS OF CHARGING PILES IN EACH PERIOD OF TNN

To provide further theoretical support for the planning of charging stations in this area, the number of charging piles required at all TNNs during the whole weekday is taken into consideration and shown in Figure 10. It is noteworthy that the statistics are on the basis of consumption that each charging pile can only serve one EV during the charging period of EVs. In other words, the statistics also reflect the number of charging EVs during the same period. Specifically, the result shows that the charging piles needed are not evenly distributed in space. The charging pile number of WA is almost 3 times more than that of RA and CA, especially during the period of 08:00 to 16:00. Additionally, this also explains the reason why the charging load of WA is much higher than that of RA and CA on weekday, as exhibited in Figure 6(a). Moreover, the demand for charging piles in RA and CA performs similarly, both of which center at the period of 16:00 to 24:00. Nevertheless, it should be noted that the charging pile demand for RA is heavier than that of CA.

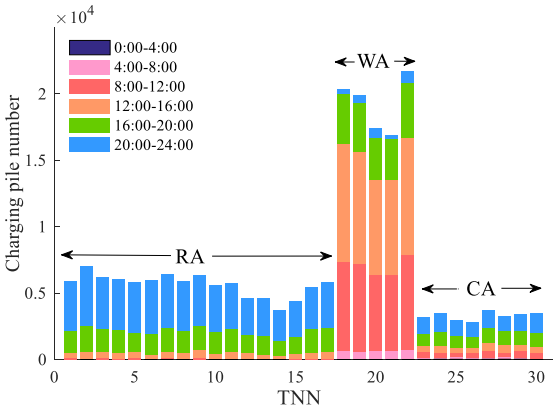

FIGURE 10. Statistics of charging piles in each period of TNNs.

F. RELATIONSHIP BETWEEN $P_{j,m}^{j+1,st}$ AND DCP

To demonstrate the impact of $P_{j,m}^{j+1,st}$ on the spatial-temporal distribution of charging load, index DCP is proposed and the simulated results are shown in Figure 11. With the increment of $P_{j,m}^{j+1,st}$, the overall reduction occurs to the DCPs of RA and CA, but an opposite trend happens to the DCP of WA. The change means that the charging load of RA and CA gradually transfers to that of WA. However, the variation interval of the three DCPs keeps within [0, 0.1]. It should be noted that the sum of the three DCPs equals to 1. Consequently, the length of the variation interval indicates that the impact of $P_{j,m}^{j+1,st}$ on the spatial-temporal distribution of charging load is limited, which reflects the stability and accuracy of the prediction method.

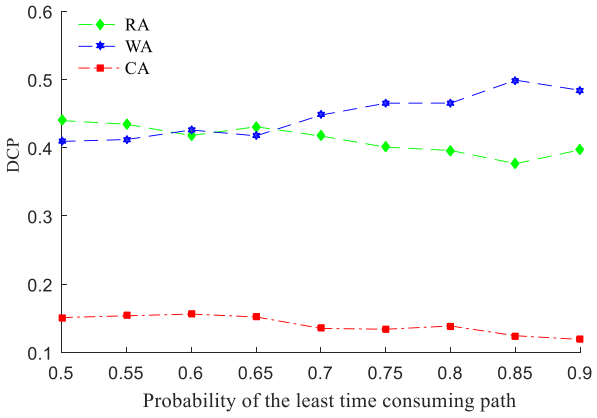

FIGURE 11. Relationship between the probability of driving time path option and the dispersion coefficient of charging load.

G. DISTRIBUTION NETWORK RELIABILITY INDEX AND LOAD LOSS

In Figure 7, It can be drawn that high temperature and congestion will lead to a higher charging load peak. To further study the impact of the two factors as well as EV penetration rate on distribution network reliability, the simulations about different EV penetration rates on weekday, high temperature day and congestion day are conducted. Table 6 gives out related reliability indices. As demonstrated in Table 6, the increment of EV penetration rates can bring bigger values of all listed indices. In addition, each reliability index on both high temperature day and congestion day is much bigger than that of weekday. This indicates that the increment of charging load can result in more fragile distribution reliability. To be technically precise, Figure 12 shows the load loss of each DNN. The results exhibit that the expanded range of DNNs with load loss and rapid growth of load loss amplitude emerge along with the rising EV penetration rates and the occurrences of high temperature and congestion. Moreover, the DNNs with load loss drop in the range of DNNs 15 to 17 and DNNs 28 to 30. It should be noted that if these DNNs are equipped with corresponding emergency power supply, the reliability of the system will be enhanced, which can provide data support for the planning of distribution network.

TABLE 6. Reliability indices of distribution network in different charging scenarios.

Charging scenarios	Reliability index			
	I_{LOLP}	I_{SAIFI} per time	I_{SAIDI}/h	I_{EENS}/MW
Penetration rate 75% on weekday	0.003273	14.5845	3.5946	36.1594
Penetration rate 87.5% on weekday	0.003371	14.9243	3.8459	39.4831
Penetration rate 100% on weekday	0.003401	15.6843	4.2137	46.1583
High temperature day	0.003513	15.9638	4.3844	55.8175
Congestion day	0.003487	15.9169	4.3233	52.7655

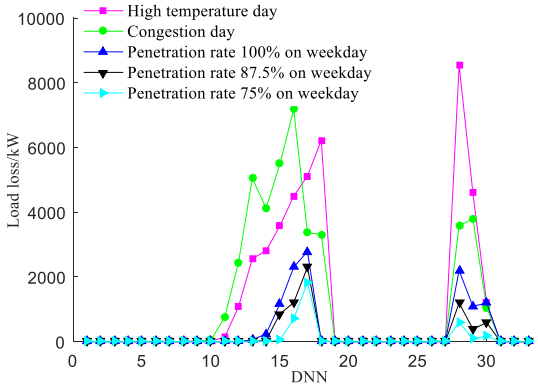

FIGURE 12. Load loss of DNNs in different charging scenarios.

H. PUV AND FVSI

To further evaluate the effect of charging load on the voltage stability of distribution network, indices including PUV and FVSI have been applied and Figure 13 displays their specific values at each DNN in different charging scenarios. Due to page limitation, Figure 13 is omitted here and interested readers are referred to supplementary material for details. It needs to be pointed out that FVSI close to 1.0 indicates that the corresponding DNN is imminent to its instability

point. In other words, the smaller value of FVSI leads to the better voltage stability of DNN. It can be obtained from Figure 13 (a)-(e) that the five charging scenarios share one commonness that a serious voltage drop happens during the period of 7:30 to 12:30 and 17:00 to 23:00. In addition, the DNNs with such serious voltage drop in these periods mainly concentrate on DNN 6-17 and 26-33. To be more technically precise, quantitative data containing the average value and minimum value of PUV is given in Table 7. It can be known from Table 7 that the increase of EV penetration rates and the emergence of high temperature and congestion will lead to the continuous decline of PUV. Similarly, from Figures 13 (f)-(j) and the average of FVSI in Table 7, it can be seen that the overall uptrend also occurs to the values of FVSI. Here, FVSI is accompanied by the rising EV penetration rates and the appearance of high temperature and congestion. In general, the decline of PUV and the growth of FVSI in the five charging scenarios indicate that the voltage stability of distribution network is debilitated to some extent.

TABLE 7. Data statistics of PUV and FVSI in different charging scenarios.

Charging scenarios	Average of PUV	Minimum PUV	Average of FVSI	Maximum FVSI
Penetration rate 75% on weekday	0.9854	0.9269	0.0293	0.3891
Penetration rate 87.5% on weekday	0.9830	0.9159	0.0302	0.4085
Penetration rate 100% on weekday	0.9772	0.8566	0.0325	0.5642
High temperature day	0.9673	0.8385	0.0361	0.5572
Congestion day	0.9708	0.8210	0.0347	0.4720

V. CONCLUSIONS AND RECOMMENDATIONS

In this paper, the spatial-temporal distribution prediction model of EV charging demand and reliability evaluation method for distribution network penetrated with EVs have been presented and analyzed. The prediction model seeks to simulate the EVs' spatial-temporal transfer randomness and path selection probability. It can precisely compute the realistic EV charging load. In addition, the reliability evaluation method enables to measure the impact of charging load in different charging scenarios with various reliability indices of distribution network. Designs and case studies have been conducted and the results can be summarized as follows:

1) Compared with Dijkstra's shortest path algorithm, the proposed prediction model fully reflects EVs' transfer randomness. Moreover, the charging load prediction results match reality much more. This is due to the reason that temperature, traffic condition and EV owner's subjective willingness have been comprehensively considered.

2) The variance of trip chain composition can result in significant distribution characteristics difference of charging load between weekdays and weekends. Moreover, both high temperature and traffic congestion will induce an amplitude increment of charging load. Additionally, the time latency of charging load also occurs on congestion day.

3) High temperature, traffic congestion and the rising EV penetration rates can undermine distribution network reliability. This can result in corresponding growth of load loss so as to guarantee the operation safety of the system.

This paper mainly focuses on the charging load prediction and corresponding reliability evaluation of distribution network. Under the premise that the number of charging piles has been determined, there may exist queuing time for charging. This is obvious in peak hours of charging demand. Its impact on the distribution of charging demand will be further simulated and discussed in detail in future work.

REFERENCES

[1] National Development and Reform Commission of China. *Guidelines for the Development of Electric Vehicle Charging Infrastructure*. Accessed: Oct. 5, 2019. [Online]. Available: http://www.ndrc.gov.cn/zcfb/zcfbtz/201511/t20151117_758762.html

[2] M. D. Galus, R. A. Waraich, F. Noembrini, K. Steurs, G. Georges, K. Boulouchos, K. W. Axhausen, and G. Andersson, "Integrating power systems, transport systems and vehicle technology for electric mobility impact assessment and efficient control," *IEEE Trans. Smart Grid*, vol. 3, no. 2, pp. 934–949, Jun. 2012.

[3] S. K. Injeti and V. K. Thunuguntla, "Optimal integration of DGs into radial distribution network in the presence of plug-in electric vehicles to minimize daily active power losses and to improve the voltage profile of the system using bio-inspired optimization algorithms," *Protection Control Mod. Power Syst.*, vol. 5, no. 1, pp. 1–5, Jan. 2020.

[4] A. Rautiainen, S. Repo, P. Jarventausta, A. Mutanen, K. Vuorilehto, and K. Jalkanen, "Statistical charging load modeling of PHEVs in electricity distribution networks using national travel survey data," *IEEE Trans. Smart Grid*, vol. 3, no. 4, pp. 1650–1659, Dec. 2012.

[5] N. H. Tehrani and P. Wang, "Probabilistic estimation of plug-in electric vehicles charging load profile," *Electr. Power Syst. Res.*, vol. 124, pp. 133–143, Jul. 2015.

[6] Z. Darabi and M. Ferdowsi, "Impact of plug-in hybrid electric vehicles on electricity demand profile," in *Smart Power Grids*. Berlin, Germany: Springer, 2012, pp. 319–349.

[7] A. Ul-Haq, C. Cecati, and E. El-Saadany, "Probabilistic modeling of electric vehicle charging pattern in a residential distribution network," *Electr. Power Syst. Res.*, vol. 157, pp. 126–133, Apr. 2018.

[8] A. Ul-Haq, M. Azhar, Y. Mahmoud, A. Perwaiz, and E. A. Al-Ammar, "Probabilistic modeling of electric vehicle charging pattern associated with residential load for voltage unbalance assessment," *Energies*, vol. 10, no. 9, pp. 1351–1368, Apr. 2017.

[9] Y. Luo, T. Zhu, S. Wan, S. Zhang, and K. Li, "Optimal charging scheduling for large-scale EV (electric vehicle) deployment based on the interaction of the smart-grid and intelligent-transport systems," *Energy*, vol. 97, pp. 359–368, Feb. 2016.

[10] Y. Shao, Y. Mu, X. Yu, X. Dong, H. Jia, J. Wu, and Y. Zeng, "A Spatial-temporal charging load forecast and impact analysis method for distribution network using EVs-traffic-distribution model," *Proc. Chin. Soc. Elect. Eng.*, vol. 37, no. 18, pp. 5207–5217, Sep. 2017.

[11] S. Su, H. Zhao, H. Zhang, X. Lin, F. Yang, and Z. Li, "Forecast of electric vehicle charging demand based on traffic flow model and optimal path planning," in *Proc. 19th Int. Conf. Intell. Syst. Appl. Power Syst. (ISAP)*, Sep. 2017, pp. 1–6.

[12] T. Chen, B. Zhang, H. Pourbabak, A. Kavousi-Fard, and W. Su, "Optimal routing and charging of an electric vehicle fleet for high-efficiency dynamic transit systems," *IEEE Trans. Smart Grid*, vol. 9, no. 4, pp. 3563–3572, Jul. 2018.

[13] S. Minelli, P. Izadpanah, and S. Razavi, "Evaluation of connected vehicle impact on mobility and mode choice," *J. Traffic Transp. Eng.*, vol. 2, no. 5, pp. 301–312, Oct. 2015.

[14] D. Tang and P. Wang, "Probabilistic modeling of nodal charging demand based on spatial-temporal dynamics of moving electric vehicles," *IEEE Trans. Smart Grid*, vol. 7, no. 2, pp. 627–636, Mar. 2016.

[15] Q. Zhang, Z. Wang, W. Tan, H. Z. Liu, and C. Li, "Spatial-temporal distribution prediction of charging load for electric vehicle based on MDP random path simulation," *Power Syst. Autom.*, vol. 42, no. 20, pp. 59–66, Oct. 2018.

[16] T. Shun, W. Jianfeng, X. Xiangning, Z. Jian, L. Kunyu, and Y. Yang, "Charging demand for electric vehicle based on stochastic analysis of trip chain," *IET Gener., Transmiss. Distrib.*, vol. 10, no. 11, pp. 2689–2698, Aug. 2016.
[17] Y. Wang and D. Infield, "Markov chain Monte Carlo simulation of electric vehicle use for network integration studies," *Int. J. Electr. Power Energy Syst.*, vol. 99, pp. 85–94, Jul. 2018.
[18] Z. Zhang, C. Liu, X. Chen, C. Zhang, and J. Chen, "Annual energy consumption of electric vehicle air conditioning in China," *Appl. Thermal Eng.*, vol. 125, pp. 567–574, Oct. 2017.
[19] G. Ferro, R. Minciardi, and M. Robba, "A user equilibrium model for electric vehicles: Joint traffic and energy demand assignment," *Energy*, vol. 198, May 2020, Art. no. 117299.
[20] L. Hong, Z. Xu, and L. Chang, "Timing interactive analysis of electric private vehicle traveling and charging demand considering the sufficiency of charging facilities," *Proc. Chin. Soc. Elect. Eng.*, vol. 38, no. 18, pp. 5469–5478, 2018.
[21] Y. Xiang, S. Hu, Y. Liu, X. Zhang, and J. Liu, "Electric vehicles in smart grid: A survey on charging load modelling," *IET Smart Grid*, vol. 2, no. 1, pp. 25–33, Mar. 2019.
[22] M. Kamruzzaman and M. Benidris, "A reliability-constrained demand response-based method to increase the hosting capacity of power systems to electric vehicles," *Int. J. Electr. Power Energy Syst.*, vol. 121, Oct. 2020, Art. no. 106046.
[23] H. Lin, Y. Liu, Q. Sun, R. Xiong, H. Li, and R. Wennersten, "The impact of electric vehicle penetration and charging patterns on the management of energy hub—A multi-agent system simulation," *Appl. Energy*, vol. 230, pp. 189–206, Nov. 2018.
[24] J.-M. Clairand, J. Rodriguez-Garcia, and C. Alvarez-Bel, "Smart charging for electric vehicle aggregators considering users' preferences," *IEEE Access*, vol. 6, pp. 54624–54635, Oct. 2018.
[25] Z. Liu, D. Wang, H. Jia, N. Djilali, and W. Zhang, "Aggregation and bidirectional charging power control of plug-in hybrid electric vehicles: Generation system adequacy analysis," *IEEE Trans. Sustain. Energy*, vol. 6, no. 2, pp. 325–335, Apr. 2015.
[26] H. Farzin, M. Moeini-Aghtaie, and M. Fotuhi-Firuzabad, "Reliability studies of distribution systems integrated with electric vehicles under battery-exchange mode," *IEEE Trans. Power Del.*, vol. 31, no. 6, pp. 2473–2482, Dec. 2016.
[27] R. Boudina, J. Wang, M. Benbouzid, F. Khoucha, and M. Boudour, "Impact evaluation of large scale integration of electric vehicles on power grid," *Frontiers Energy*, vol. 14, no. 2, pp. 337–346, Apr. 2018.
[28] Q. Zhang, Y. Zhu, Z. Wang, Y. Su, and C. Li, "Reliability assessment of distribution network and electric vehicle considering quasi-dynamic traffic flow and Vehicle-to-Grid," *IEEE Access*, vol. 7, pp. 131201–131213, Sep. 2019.
[29] G. Liu, L. Kang, Z. Luan, J. Qiu, and F. Zheng, "Charging station and power network planning for integrated electric vehicles (EVs)," *Energies*, vol. 12, no. 13, p. 2595, Jul. 2019.
[30] C. Caro-Ruiz, A. S. Al-Sumaiti, S. Rivera, and E. Mojica-Nava, "A MDP-based vulnerability analysis of power networks considering network topology and transmission capacity," *IEEE Access*, vol. 8, pp. 2032–2041, 2020.
[31] C. Liu, J. Wang, W. Cai, and Y. Zhang, "An energy-efficient dynamic route optimization algorithm for connected and automated vehicles using velocity-space-time networks," *IEEE Access*, vol. 7, pp. 108866–108877, 2019.
[32] Y. Xiang, Z. Jiang, C. Gu, F. Teng, X. Wei, and Y. Wang, "Electric vehicle charging in smart grid: A spatial-temporal simulation method," *Energy*, vol. 189, Dec. 2019, Art. no. 116221.
[33] E. Yao, Z. Yang, Y. Song, and T. Zuo, "Comparison of electric vehicle's energy consumption factors for different road types," *Discrete Dyn. Nature Soc.*, vol. 2013, pp. 1–7, Dec. 2013.
[34] S. Sun, Q. Yang, and W. Yan, "Optimal temporal-spatial PEV charging scheduling in active power distribution networks," *Protection Control Mod. Power Syst.*, vol. 2, no. 1, p. 34, Sep. 2017.
[35] S. Sulaeman, Y. Tian, M. Benidris, and J. Mitra, "Quantification of storage necessary to firm up wind generation," *IEEE Trans. Ind. Appl.*, vol. 53, no. 4, pp. 3228–3236, Jul. 2017.
[36] M. K. Meena and N. Kumar, "On-line monitoring and simulation of transmission line network voltage stability using FVSI," in *Proc. 2nd IEEE Int. Conf. Power Electron., Intell. Control Energy Syst. (ICPEICES)*, Oct. 2018, pp. 257–260.
[37] W. Wei, Y. Zhou, J. Zhu, K. Hou, H. Zhao, Z. Li, and T. Xu, "Reliability assessment for AC/DC hybrid distribution network with high penetration of renewable energy," *IEEE Access*, vol. 7, pp. 153141–153150, 2019.
[38] S. Su, Y. Hu, L. He, K. Yamashita, and S. Wang, "An assessment procedure of distribution network reliability considering photovoltaic power integration," *IEEE Access*, vol. 7, pp. 60171–60185, 2019.
[39] S. Cheng, Y. Feng, and X. Wang, "Application of Lagrange relaxation to decentralized optimization of dispatching a charging station for electric vehicles," *Electronics*, vol. 8, no. 3, p. 288, Mar. 2019.

SHAN CHENG (Member, IEEE) received the M.S. and Ph.D. degrees from the School of Electric Engineering, Chongqing University, China, in 2013. He is currently an Associate Professor with the College of Electrical Engineering and New Energy, China Three Gorges University. His research interests include power system optimization, smart grid energy management and operation optimization and control, and intelligent optimization algorithm and its application to power systems.

ZHAOBIN WEI was born in Sichuan, China, in 1995. He received the bachelor's degree from Xihua University, in 2018. He is currently pursuing the master's degree with China Three Gorges University. His research interests include application of decentralization optimization in power systems and power system reliability assessment.

DONGDONG SHANG was born in Hubei, China, in 1997. He received the bachelor's degree from the Wuhan University of Science and Technology City College, in 2019. He is currently pursuing the master's degree with China Three Gorges University. His research interests include optimized operation of active distribution network with electric vehicles and power system reliability assessment.

ZIKAI ZHAO was born in Henan, China, in 1997. He received the bachelor's degree from the Henan University of Science and Technology, in 2019. He is currently pursuing the master's degree with China Three Gorges University. His research interests include application of decentralization optimization in power systems and power system reliability assessment.

HUIMING CHEN received the B.Eng. degree (Hons.) in electronic engineering from Sichuan University, in 2014, and the M.Phil. degree from the Department of Electrical and Electronic Engineering, The University of Hong Kong (HKU), in 2016. where he is currently the Ph.D. degree. He has published several IEEE transaction articles and international conference papers. His current research interests include statistical signal processing and stochastic optimization, with applications in machine learning and wireless communication systems.